Bulgarian Chemical Communications, Volume 50, Special Issue G (pp. 78 - 85) 2018

Atmospheric dispersion modelling and radiological safety analysis for a hypothetical accident of liquid-fuel thorium molten salt reactor (TMSR-LF)

Bo Cao[1, 2, 3*], Weijie Cui[1, 2], Irsa Rasheed[1, 2], Yixue Chen[1, 2]

[1]*School of Nuclear Science and Engineering, North China Electric Power University, Beijing, 102206, China*

[2]*Beijing Key Laboratory for Passive Safety Technology of Nuclear Energy, North China Electric Power University, Beijing, 102206, China*

[3] *Departments of Atmospheric and Oceanic Sciences, University of California, Los Angeles, CA, 90095, USA*

The molten salt reactor (MSR) is one of the six advanced reactor types for future nuclear energy proposed in the Generation IV International Forum (GIF). Because of its potentially favourable economic, fuel utilization, and safety characteristics and nuclear proliferation resistance, the MSR has aroused widespread concern in recent years. Indeed, from 2011, the Shanghai Institute of Applied Physics started the "Thorium Molten Salt Reactor Nuclear Energy System (TMSR)" project in China and aimed to construct a liquid-fuel thorium molten salt reactor (TMSR-LF) and a solid-fuel thorium molten salt reactor (TMSR-SF). An optimized 2 MWth TMSR-LF has been designed and will be built recently in Gansu province. In this study, HotSpot health physics computer code has been used for atmospheric dispersion modelling and radiological safety assessment considering site-specific meteorological conditions. Calculations for total effective dose equivalent (TEDE), ground deposition and the respiratory time-integrated air concentration have been performed, with results indicating maximum value of ground deposition equal to 2.5E+01kBq/m^{2}at a distance of 0.6km from the reactor. Maximum value of TEDE falls below the public dose limit of 1mSv/year proposed by ICRP even for the worst case accident scenario as set in IAEA safety Report Series number 115. The TEDE has three components: inhalation, ground shine and air submersion, the submersion and ground shine doses are insignificant compared to the inhalation doses. It is observed that the highest value of committed effective dose equivalent (CEDE) appears to be the lung, the lower large intestine wall appears to be the second most exposed organ, followed by upper large intestine wall and the red marrow, respectively. The contribution of total 18 selected radionuclides was investigated, three main radionuclides including Sr-90, Sr-89, Cs-137 are the main contributors to the CEDE.

Keywords: atmospheric dispersion modelling, radiological safety analysis, TMSR-LF, TEDE, HotSpot

INTRODUCTION

Generation IV International Forum (GIF) has anticipated molten salt reactor (MSR) as one of the advanced reactors to fulfil the future nuclear energy demands [1], owing to its economic fuel utilization, nuclear proliferation resistance and advanced safety characteristics [2-6].

The MSR was first developed in the Oak Ridge National Laboratory (ORNL) in the late 1940s. The first Molten Salt Reactor Experiment (MSRE) began to construct in 1962 and operated at full power in December 1966 [7]. Several conceptual designs of the MSR have been proposed and have been studied in the past 60 years. Japan, Russia and other countries also paid much attention to the MSR [4, 8-10]. In China, the Shanghai Institute of Applied Physics started the "Thorium Molten Salt Reactor Nuclear Energy System (TMSR)" project in China and aimed to construct a liquid-fuel thorium molten salt reactor (TMSR-LF) and a solid-fuel thorium molten salt reactor (TMSR-SF).

An optimized 2 MWth TMSR-LF has been designed and will be built in Gansu province recent years. For a MSR, as a fluid fuel reactor, on-line fuel processing can be applied, which helps in removal of gaseous and volatile parts from the source term [7, 11]. The MSR is a more safety advanced reactor and is more resistant to consequences of large accidents in comparison to other reactor types, but there is risk for the source term may be released to the environment [3-5]. It is still necessary to predict the radiological safety analysis of a hypothetical accident with the radionuclides available for release to the environment.

Radiological safety analysis for hypothetical accident provides a major contribution for the safety analysis of nuclear power plant, as far as human health and safety is concerned [12-20].

The total effective dose equivalent (TEDE) attributes to both internal and external dose equivalents for the body resulting from the release of radionuclides during accident. Thus, TEDE is computed by addition of both effective dose equivalent (EDE) and the total committed effective dose equivalent (CEDE). The EDE was caused by the external material such as submersion, ground shine and resuspension, and CEDE was caused by

* To whom all correspondence should be sent:
caobo@ncepu.edu.cn

the internal material such as inhalation. The TEDE is the most complete expression of the combined dose from all applicable delivery pathways [20, 21].

Lawrence Livermore National Laboratory (LLNL) has established a HotSpot computer code for the analysis of personnel health physics near the reactor sites. Gaussian Plume Model (GPM) has been employed for HotSpot code for the calculation of air concentration and TEDE due to release of radionuclides into the atmosphere [21]. In practice, the GPM is one of the most widely validated general dispersion models and has been successfully applied in various dispersion problems [13-20].

In this work, we have performed the atmospheric dispersion modelling and radiological safety analysis of a hypothetical TMSR-LF accident by HotSpot health physics computer code considering site-specific meteorological conditions. The TEDE, the respiratory time-integrated air concentration, and the ground deposition are calculated with source term including 18 radionuclides. These results provide reference for the assessment source term of emergency facility and offsite consequence assessment.

MATERIALS AND METHOD

Site-specific conditions of the TMSR-LF

The TMSR-LF will be in the Wuwei City, Gansu Province, China. It will be built about 2020. Wuwei city has a temperate continental arid climate, where evaporation is larger than precipitation. The local meteorological data indicate a mean year rainfall is about 60~610 mm and a mean year evaporation is about 1400~3040 mm. North-North-West (NNW) and West-South-South (WSS) are the predominant directions, which occurred for about 49.1% and 10.4% with an average speed of 5.0m/s and 2.0m/s, respectively. Stability class D gains predominance as it has percentage occurrence of 61.2%, the second being the stability class E with percentage occurrence of 9.3%, and the remaining 29.5% is taken by other classes.

Source term and accidental release scenario

The TMSR-LF is a graphite moderated reactor. The thermal power is 2 MW, and the fuel salt is LiF-BeF_2-ThF_4-UF_4 (68-28-0.1-3.9 mol %) with 99.95 % abundance of ^7Li and a coolant salt of LiF-NaF-KF [2, 6].

Although MSR has some inherent features compared with other reactor systems, it still has some safety disadvantage, including the accumulation of fission products in different parts like the primary system, the off-gas system, the fuel storage tanks, and the processing plant. This highlights the significance for proper containment of fission products and removal of decay heat under all anticipated circumstances [11]. According to the research, off-gas system failure accident is generally recognized as the most likely path for radiation release [4, 5]. Base on it, in this paper, the source term is mainly contributed by the off-gas system failure and the radioactivity leak by reactor vessel and pipes. The accident source term during 0~ 1 hour for TMSR-LF is shown in Tab.1 [6].

Table 1: Accident source term for TMSR-LF

Nuclide	Activity released / Bq
H-3	3.30×10^{12}
Kr-85	8.75×10^{4}
Kr-85m	1.28×10^{6}
Kr-87	1.45×10^{7}
Kr-88	1.03×10^{7}
Xe-133	2.48×10^{4}
Xe-135	4.17×10^{6}
I-131	1.51×10^{7}
I-132	2.83×10^{6}
I-133	3.54×10^{7}
I-134	1.15×10^{8}
I-135	6.96×10^{8}
Cs-134	4.21×10^{6}
Cs-137	1.63×10^{10}
Sr-89	5.29×10^{11}
Sr-90	8.46×10^{10}
Ru-103	8.38×10^{5}
Ru-106	1.89×10^{5}

The release height was assumed at 40 m and buoyancy and exit momentum effects were neglected. Depending on the site meteorology, a downwind transportation of radionuclides happens after the accident. The annual average wind speed at 10 m is 5 m/s in the predominant direction of NNW. Stability class D gains predominance because of its largest percentage occurrence of 61.2%, a default value of 1.7m for the receptor height and value of 1300m for the inversion layer height has been chosen. A value of 3.33×10^{4} m^3 s/l

has been used for the breathing rate of an average human being.

RESULTS AND DISCUSSION

TEDE results and analysis

Based on the site-specific meteorological conditions, an assessment for the calculation of radiation dose calculation was done by HotSpot 3.03 after the hypothetical accident. The TEDE, the ground deposition and the respiratory time-integrated air concentration were generated as a function of downwind distance as presented in Tab.2. It can be seen from Tab.2 that the maximum TEDE is 1.6E-04 Sv at the downwind distance of 0.6 km, which is also shown in Fig.1. It is far below the annual regulatory limits of 1 mSv from public exposure in a year even in the event of worse accident scenario as set in IAEA Safety Report Series number 115, no action related specifically to the public exposure is required.

Meanwhile, the maximum respiratory time-integrated air concentration and the ground deposition value of 5.2E+07 Bq-s/m^3 and 2.5E+01 kBq/m^2 occurred at 0.6 km at an arrival time about one minutes. As is shown in Fig.1 the TEDE first increases with increasing distance downwind, reaches the maximum value and then decreases. The plume centreline ground deposition of radionuclides as a function of downwind distance is shown in Fig.2, which shows a similar tend as TEDE shown in Fig.1. The maximum value of plume centreline ground deposition is 2.5E+01 kBq/m^2 occurred at about 0.6 km from the reactor, which is accordance with results shown in Tab.2.

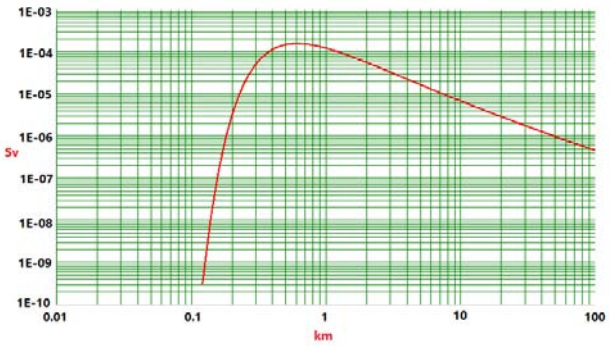

Fig.1. TEDE as a function of downwind distance from the NPP site in D class

Table 2. Downwind distance and other plume parameters at different arrival time intervals

Distance/km	TEDE/Sv	Respirable time-integrated air concentration/ Bq-sm^{-3}	Ground surface deposition/ kBqm^{-2}	Ground shine dose rate/ Svh^{-1}	Arrival time /h: min
0.03	0.00E+00	0.00E+00	0.00E+00	0.00E+00	<00:01
0.1	4.7E-13	1.5E-01	1.7E-08	1.2E-18	<00:01
0.2	3.2E-06	1.0E+06	4.3E-01	2.9E-11	<00:01
0.3	5.1E-05	1.7E+07	7.7E+00	5.2E-10	<00:01
0.4	1.1E-04	3.7E+07	1.8E+01	1.2E-09	0:01
0.5	1.5E-04	4.9E+07	2.3E+01	1.6E-09	0:01
0.6	1.6E-04	5.2E+07	2.5E+01	1.7E-09	0:01
0.7	1.5E-04	5.1E+07	2.4E+01	1.6E-09	0:01
0.8	1.4E-04	4.8E+07	2.3E+01	1.5E-09	0:02
0.9	1.3E-04	4.4E+07	2.1E+01	1.4E-09	0:02
1	1.2E-04	4.0E+07	1.0E+01	1.3E-09	0:02
2	5.6E-05	1.9E+07	8.8E+00	6.0E-10	0:05
4	2.2E-05	7.5E+06	3.5E+00	2.4E-10	0:10
6	1.3E-05	4.4E+06	2.1E+00	1.4E-10	0:16
8	9.0E-06	3.0E+06	1.4E+00	9.6E-11	0:21
10	6.8E-06	2.3E+06	1.1E+00	7.2E-11	0:27
20	2.9E-06	9.9E+05	4.5E-01	3.0E-11	0:54
40	1.3E-06	4.5E+05	2.0E-01	1.3E-11	1:48
60	8.0E-07	2.9E+05	1.3E-01	8.3E-12	2:42
80	5.8E-07	2.1E+05	9.2E-02	6.0E-12	03:36

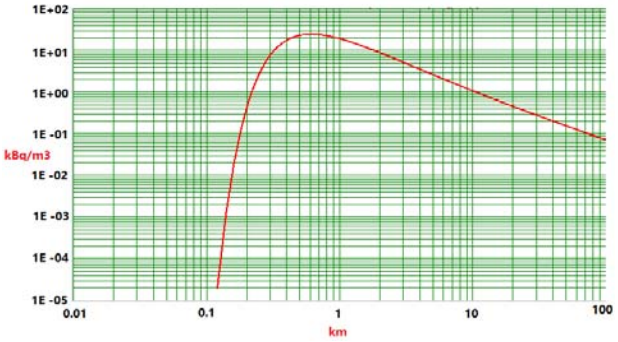

Fig.2. Plume centreline ground deposition of radionuclides as a function of downwind distance in D class

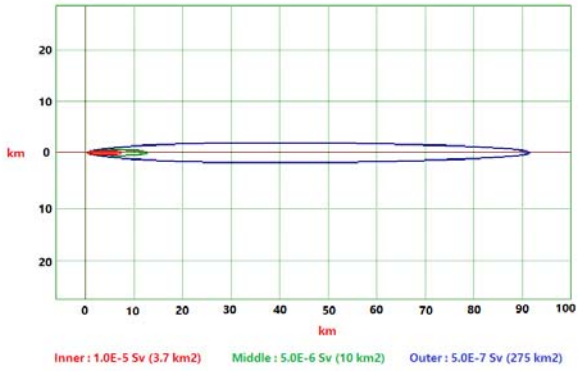

Fig.3. TEDE counter plot for D class

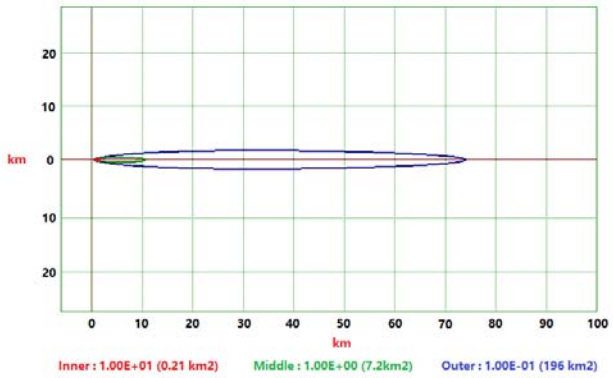

Fig.4. Plume contour ground deposition distribution for D class

Table 3. TEDE including inhalation and submersion and ground shine in different distance

Distance/ km	TEDE/Sv	Inhalation /Sv	Submersion/ Sv	Ground Shine/Sv
0.03	0.00E+00	0	0	0
0.1	4.7E-13	4.69E-13	2.21E-17	2.33E-18
0.2	3.2E-06	3.19E-06	1.50E-10	5.70E-11
0.3	5.1E-05	5.06E-05	2.38E-09	1.03E-09
0.4	1.1E-04	1.14E-04	5.35E-09	2.37E-09
0.5	1.5E-04	1.48E-04	6.95E-09	3.10E-09
0.6	1.6E-04	1.57E-04	7.39E-09	3.30E-09
0.7	1.5E-04	1.53E-04	7.21E-09	3.23E-09
0.8	1.4E-04	1.44 E-04	6.77E-09	3.03E-09
0.9	1.3E-04	1.33E-04	6.25E-09	2.80E-09
1	1.2E-04	1.22E-04	5.73E-09	2.57E-09
2	5.6E-05	5.58E-05	2.62E-09	1.18E-09
4	2.2E-05	2.24E-05	1.05E-09	4.72E-10
6	1.3E-05	1.31E-05	6.13E-10	2.75E-10
8	9.0E-06	9.00E-06	4.21E-10	1.89E-10
10	6.8E-06	6.78E-06	3.16E-10	1.42E-10
20	2.9E-06	2.87E-06	1.33E-10	6.00E-11
40	1.3E-06	1.27E-06	5.84E-11	2.64E-11
60	8.0E-07	8.00E-07	3.64E-11	1.65E-11
80	5.8E-07	5.79E-07	2.61E-11	1.19E-11

In addition, Fig.3 and Fig.4 show TEDE contour plot and plume contour ground deposition distribution under the plume for stability class D and wind speed of 5 m/s, respectively. It can be seen from Fig.3 that three regions with the area of 3.7, 10 and 275 km^2 has been marked with dose contours of 1.00E-05, 5.00E-06 and 5.00E-07 Sv. Moreover, as is shown in Fig.4, three regions with the area of 0.21, 7.2 and 196 km^2 has been marked with deposition contours of 10, 1 and 0.1 kBq/m^2. The TEDE and plume contour ground deposition distribution move away from the source as a function of downwind distance. The red colour area shows higher dose risk for personnel and population, the green and blue area are safer compared with red area. According to the above results and analysis, the calculated TEDE in all distances is below the maximum public dose limit proposed by ICRP, thus reducing the risk for serious hazards for the personnel and population.

Based on the situation, multiple pathways are available for the radiation absorptions, for example TEDE includes the plume passage inhalation and submersion and ground shine which is shown in

Tab.3. It is very obviously that the plume passage inhalation is biggest the donation among them. Moreover, the CEDE is mainly caused by the internal material because of inhalation.

Organ CEDE results and analysis

CEDE specifies the committed dose equivalent, which includes dose equivalents for internal body organ or tissues, which have absorbed radiaton over a period of 50 years after the intake of radioactive material. In HotSpot also, CEDE is calculated by the traditional method, that is by integrating the committed dose equivalents throughout 50 years for different tissues and organs of the body, and an appropriate multiplication factor W_T has been used for each committed dose equivalent.

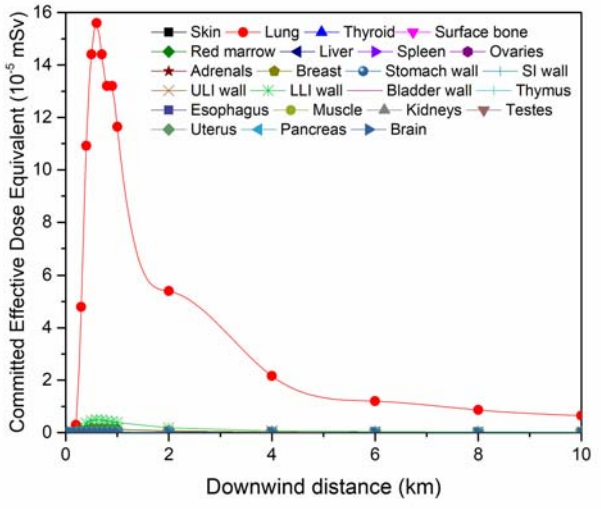

Fig.5. Organ CEDE profile due to 18 selected nuclides versus downwind distance (LLI: lower large intestine; SI: small intestine; ULI: upper large intestine)

Fig.5 and Fig.6 show the distribution of CEDE to different organs as a function of downwind distance. It can be seen from Fig.5 that the biggest value of organ CEDE appears to be the lung. The maximum CEDE of the lungs is about 1.56E-4 Sv at the downwind distance of 0.6 km. Meanwhile, Fig.6 shows the other organs CEDE as a function of downwind distance except for lungs, because the CEDE of the lungs is far larger that others. From Fig.5 and Fig.6, the lung tops the list, followed by the lower large intestine (LLI) wall, upper large intestine (ULI) wall and red marrow, respectively. It is concluded that these four organs are more radiation sensitive than the others. All the target organ CEDE plots are similar Gaussian trend, as they deplete with as they deplete with distance from receptor location. The maximum CEDE of LLI wall, ULI wall and red marrow are about 4.92E-6, 1.68E-6 and 1.56E-6 Sv at the downwind distance of 0.6 km, respectively.

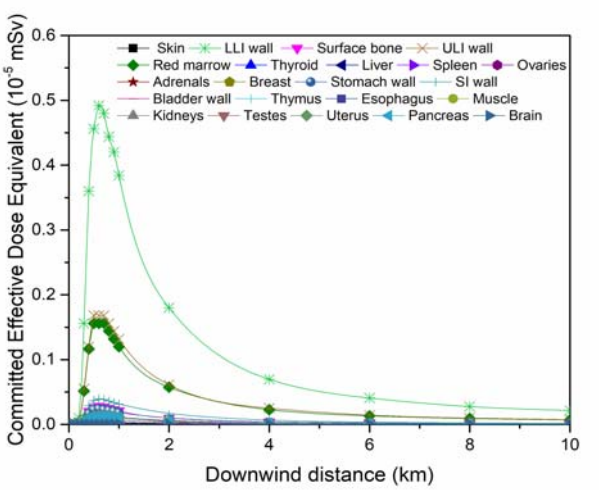

Fig.6. Organ CEDE profile due to 18 selected nuclides versus downwind distance (LLI: lower large intestine; SI: small intestine; ULI: upper large intestine; not include lung)

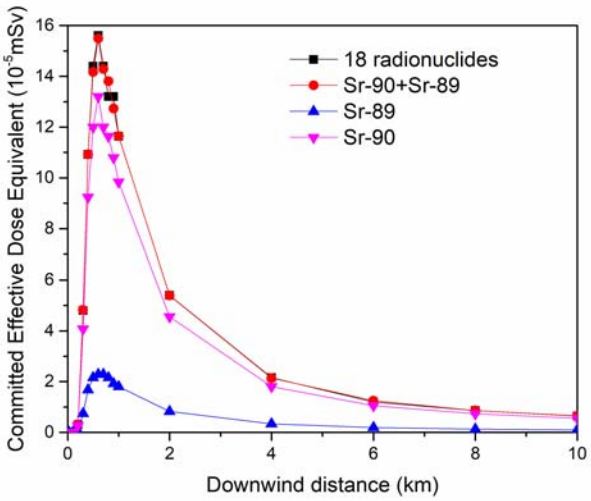

Fig.7. Lung CEDE profile versus downwind distance

The biological properties of the main contributors to the lung CEDE are Sr-90 and Sr-89, which is shown in Fig.7. These two radionuclides are responsible for such a CEDE plot trend, others are very little contributors. Because the lung CEDE contribution percentage of Sr-90 and Sr-89 are about 84.6% and 14.6% at the maximum CEDE. Fig.8 shows the LLI wall CEDE profile as a function of downwind distance. The biological properties of the main contributors to the LLI wall CEDE are Sr-89, Sr-90 and Cs-137, responsible for the dose are about 78%, 19%, and 1.6% at the maximum CEDE, respectively.

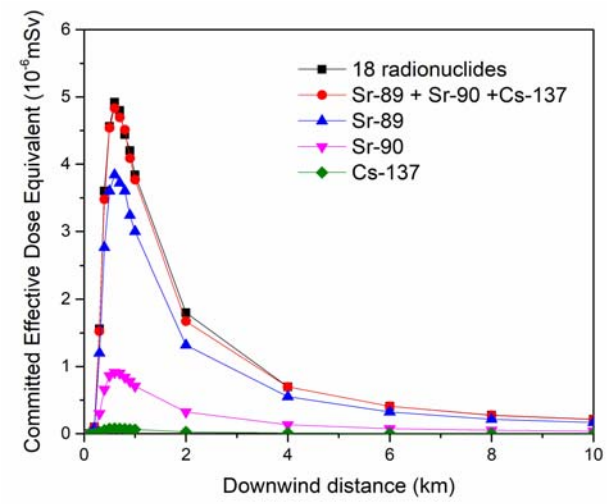

Fig.8. LLI wall CEDE profile versus downwind distance

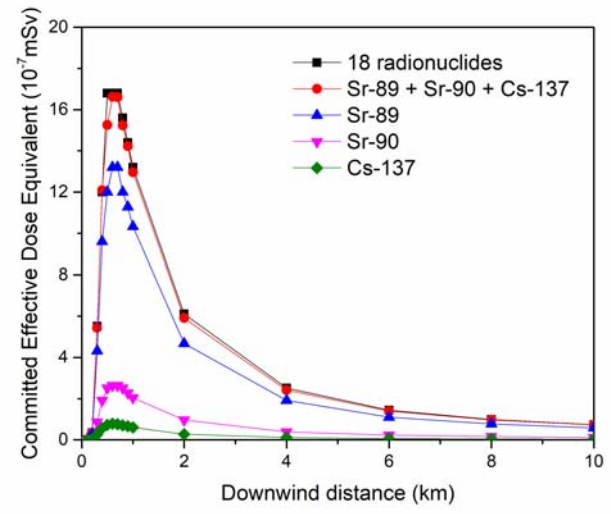

Fig.9. ULI wall CEDE profile versus downwind distance

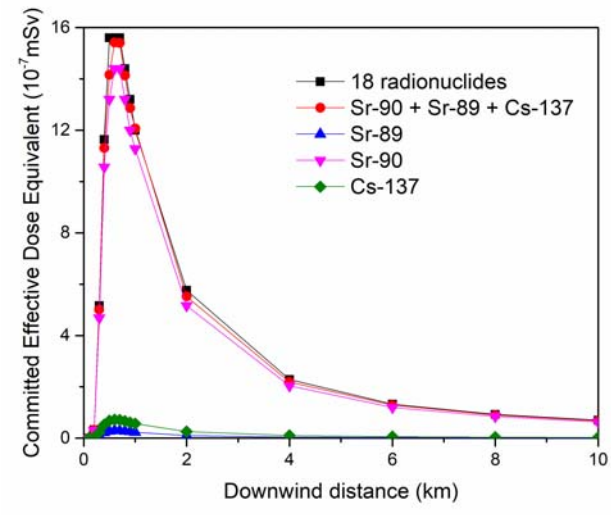

Fig.10. Red Marrow CEDE profile versus downwind distance

Fig.9 and Fig.10 show the ULI wall and red marrow CEDE profile as a function of downwind distance, respectively. The biological properties of the main contributors to the ULI wall and red marrow CEDE are Sr-89, Sr-90 and Cs-137, similar to the LLI wall. For the ULI wall CEDE, Sr-89 is the top contributor, followed by Sr-90 and Cs-137. But for the red marrow CEDE, the biggest contributor is Sr-90 at the maximum CEDE, followed by Cs-137 and Sr-89.

From the above results and analysis, we can conclude that three radionuclides including Sr-90, Sr-89, Cs-137 are the main contributors to the CEDE. Sr-90 is a bone-seeking radionuclide that exhibits biochemical behaviour similar to calcium, the next lighter group 2 elements. It is preferentially incorporated into bones and teeth and will result in long-lasting exposure to ionizing radiation. In addition to this, absorption of rays from radioactive strontium can cause cancers of the bone, bone marrow, and soft tissues around the bone. Cs-137 has gained special attention because of its highest yield percentage, intermediate half-life, high-energy radioactivity, and chemical reactivity. Moreover, it was found as a major health concern in Chernobyl and Fukushima nuclear accident. After penetrating the body, caesium gets uniformly distributed through the body particularly in soft tissues, thus indicating a serious health hazard. It is recommended to take precautionary measures to avoid inhalation and ingestion in case of accidents.

CONCLUSIONS

In this article, the radiation dose calculations and radiological consequences of a hypothetical accident have been performed by considering the TMSR-LF the off-gas system failure and the radioactivity leak by reactor vessel and pipes accident by HotSpot code 3.03. After the hypothetical TMSR-LF accident, TEDE, the respiratory time-integrated air concentration and the ground deposition are calculated. The maximum TEDE value of 1.6E-04 Sv and the maximum plume centreline ground deposition value of 2.5E+01 kBq/m^2 occurred at 0.6 km from the reactor, which is below the maximum public dose limit of 1 mSv/year as mentioned in IAEA Safety Report Series No.115. The inhalation doses are significant components of the TEDE compared with the submersion and ground shine doses. It is observed that the highest value of CEDE appears to be the lung, the lower large intestine wall appears to be the second most exposed organ, followed by upper large intestine wall and the red marrow,

respectively. The contribution of total 18 selected radionuclides was investigated, three main radionuclides including Sr-90, Sr-89, Cs-137 are the main contributors to the CEDE.

ACKNOWLEDGEMENTS

This research was financially supported by National Natural Science Foundation of China (11605059), the Fundamental Research Funds for the Central Universities (2018MS042) and China Scholarship Council (CSC).

NOMENCLATURE

MSR - molten salt reactor;
GIF - Generation IV International Forum;
ORNL - Oak Ridge National Laboratory;
MSRE - Molten Salt Reactor Experiment;
TMSR - Thorium Molten Salt Reactor Nuclear Energy System;
TMSR-LF - liquid fuel molten salt reactor;
TMSR-SF - solid fuel molten salt reactor;
TEDE - total effective dose equivalent;
EDE - effective dose equivalent;
CEDE -total committed effective dose equivalent;
LLNL - Lawrence Livermore National Laboratory;
GPM - Gaussian plume model;
NNW - North-North-West;
WSS - West-South-South;
IAEA - International Atomic Energy Agency;
ICRP - International Commission for radiation protection;
WT - weighting factors;
LLI - lower large intestine;
SI - small intestine;
ULI - upper large intestine.

REFERENCES

[1] DoE, U. S., 2002, A technology roadmap for Generation IV Nuclear Energy Systems. *Nuclear Energy Research Advisory Committee and the Generation IV International Forum*, *United States Department of Energy, Washington, DC*, 42–47 (2002).

[2] X.W. Lyu, X.B. Xia, Z. H. Zhang, J. Cai, C.Q. Chen, Analysis of tritium production in a 2 MW liquid-fueled molten salt experimental reactor and its environmental impact. *Nuclear Science and Techniques* **27**, 78 (2016).

[3] B.M. Elsheikh, Safety assessment of molten salt reactors in comparison with light water reactors. *Journal of Radiation Research and Applied Sciences* **6**, 63-70 (2013).

[4] R. Yoshioka1, K. Mitachi, Y. Shimazu, M. Kinoshita, Safety criteria and guidelines for MSR accident analysis. *Proc. Of the international conference on physics of reactors (PHYSOR2014), Kyoto, CD-ROM* (2014).

[5] D.W. Hummel, Source term evaluation for advanced small modular reactor concepts. Proc. of ITMSR-4, 4th int. conf on Small Reactors, *Ottawa,* (2016).

[6] X.W. Lyu, Radiological environmental impact analysis of airborne radioactive effluents from 2 MW thorium molten salt reactor with liquid fuel. Doctor degree, China, (2016).

[7] M.W. Rosenthal, Molten salt reactors–history, status, and potential, *Nuclear Applications and Technology*, **8**, 102-113 (1970).

[8] K Mitachi, Y. Yamana, T. Suzuki, K. Furukawa. Neutronic examination on plutonium transmutation by a small molten-salt fission power station technical report. IAEA-TECDOC–840, 1995.

[9] **S.** Jérôme, A. Michel, B. Ondřej D. Sylvie F. Olga, G. Véronique, H. Daniel, H. David, I. Victor, L . K. Jan, L. Lelio, M.L. Elsa, U. Jan, Y. Ritsuo, Z.M. Dai. The molten salt reactor (MSR) in generation IV: overview and perspectives. *Progress in Nuclear Energy* **77**, 308-319 (2014).

[10] V. Ignatiev. MOSART fuels and container materials study: case for Na, Li, Be/F solvent system. *Proceedings of the 2003 ANS/ENS International Winter Meeting (GLOBAL 2003)*, *New Orleans, LA.* (2003).

[11] S.E. Beall, P.N. Haubenreich, R.B. Lindauer and J.R. Tallackson, MSRE Design and Operation Report Part V Reactor Safety Analysis Report. Oak Ridge National Laboratory report ORNL-TM-732, 1964.

[12] A. Pirouzmand, P. Dehghani, K. Hadad, M. Nematollahi. Dose assessment of radionuclides dispersion from Bushehr nuclear power plant stack under normal operation and accident conditions. *International Journal of Hydrogen Energy* **40 (44)**, 15198-15205 (2015).

[13] S. S. Raza, M. Iqbal. Atmospheric dispersion modelling for an accidental release from the Pakistan Research Reactor-1 (PARR-1). *Annals of Nuclear Energy* **32**, 1157–1166 (2005).

[14] S.A. Birikorang, R.G. Abrefah, R.B.M. Sogbadji, B.J.B. Nyarko, J.J. Fletcher, E.H.K. Akaho. Ground deposition assessment of radionuclides following a hypothetical release from Ghana Research Reactor-1 (GHARR-1) using atmospheric dispersion model. *Progress in Nuclear Energy* **79**, 96–103 (2015).

[15] N. Sadeghi, M. Sadrnia, S. Khakshournia. Radiation dose calculations for an accidental release from the Tehran Research Reactor. *Nuclear Engineering and Design* **257**, 67–71 (2013).

[16] J.L. Muswema, G.B. Ekoko, V.M. Lukanda, J.K.-K. Lobo, E.O. Darko, E.K. Boafo. Source term derivation and radiological safety analysis for the TRICO II research reactor in Kinshasa. *Nuclear Engineering and Design* **281**, 51–57 (2015).

[17] J.L. Muswema, G.B. Ekoko, V.M. Lukanda, J.K.-K. Lobo, V. M. Lukanda, E.K. Boafo. TRICO II Core Inventory Calculation and its Radiological Consequence Analyses. *Journal of Nuclear Engineering and Radiation Science* **2**, 024501 (2016).

[18] A. Anvar, L. Safarzadeh. Assessment of the total effective dose equivalent for accidental release from the Tehran Research Reactor. *Annals of Nuclear Energy* **50**, 251–255 (2012).

[19] J.L. Muswema, E.O. Darko. Atmospheric dispersion modelling and radiological safety analysis for a hypothetical accident of Ghana Research Reactor-1 (GHARR-1). *Annals of Nuclear Energy* **68 (3)**, 239–246 (2014).

[20] B. Cao, J.X. Zheng, Y.X. Chen. Radiation Dose Calculations for a Hypothetical Accident in Xianning Nuclear Power Plant. *Science and Technology of Nuclear Installations* **2016,** 3105878 (2016).

[21] S. G. Homann, F.Aluzzi, HotSpot Health Physics Code, Version 3.0, User's Guide, LLNL-SM-636474. National Atmospheric Release Advisory Center, Lawrence Livermore National Laboratory, Livermore, CA 94550, 2013.